

Excess conductivity of  $\text{Cu}_{0.5}\text{Tl}_{0.5}\text{Ba}_2\text{Ca}_1\text{Cu}_2\text{O}_{8-\delta}$  thin films induced by thermal fluctuation: importance of 3D fluctuations

This article has been downloaded from IOPscience. Please scroll down to see the full text article.

2008 J. Phys.: Condens. Matter 20 045216

(<http://iopscience.iop.org/0953-8984/20/4/045216>)

View [the table of contents for this issue](#), or go to the [journal homepage](#) for more

Download details:

IP Address: 129.252.86.83

The article was downloaded on 29/05/2010 at 08:04

Please note that [terms and conditions apply](#).

# Excess conductivity of $\text{Cu}_{0.5}\text{Tl}_{0.5}\text{Ba}_2\text{Ca}_1\text{Cu}_2\text{O}_{8-\delta}$ thin films induced by thermal fluctuation: importance of 3D fluctuations

A A Khurram and Nawazish A Khan

Materials Science Laboratory, Department of Physics, Quaid-i-Azam University, Islamabad 45320, Pakistan

Received 5 August 2007, in final form 5 December 2007

Published 8 January 2008

Online at [stacks.iop.org/JPhysCM/20/045216](http://stacks.iop.org/JPhysCM/20/045216)

## Abstract

The superconductivity in  $\text{Cu}_{0.5}\text{Tl}_{0.5}\text{Ba}_2\text{Ca}_1\text{Cu}_2\text{O}_{8-\delta}$  ( $\text{Cu}_{0.5}\text{Tl}_{0.5}$ -1212) thin films is studied in the light of the Aslamazov–Larkin (AL) theory of fluctuation-induced conductivity (FIC). Analysis of FIC has shown that removal/addition of oxygen in the charge reservoir layer after post-annealing of  $\text{Cu}_{0.5}\text{Tl}_{0.5}$ -1212 thin films changes the dimensionality of the fluctuations which induce conductivity of mobile carriers. The samples post-annealed in nitrogen have shown higher  $T_c(0)$  with 3D behavior of FIC over a wide temperature range, whereas the samples post-annealed in oxygen have smaller  $T_c(0)$  and possess only 2D fluctuations. These results suggest that the value of  $T_c(0)$  also depends on the dimensionality of thermal fluctuations which induce excess conductivity.

## 1. Introduction

The zero resistivity critical temperature ( $T_c(0)$ ) of oxide high temperature superconductors is very much sensitive to carrier concentration in  $\text{CuO}_2$  planes. The maximum  $T_c(0)$  in a particular superconductor of a homologous series is achieved only when the carrier concentration in  $\text{CuO}_2$  planes is optimum, i.e. 0.2 holes/ $\text{CuO}_2$  plane [1–6]. There are two methods which control the carrier concentration. One is the addition (removal) of oxygen in the sample by post-annealing in an oxygen/nitrogen atmosphere, called the self-doping method, and the second is the substitution of a suitable element in the charge reservoir layer. We have chosen the self-doping method for modifying carrier concentration in  $\text{Cu}_{0.5}\text{Tl}_{0.5}\text{Ba}_2\text{Ca}_1\text{Cu}_2\text{O}_{8-\delta}$  ( $\text{Cu}_{0.5}\text{Tl}_{0.5}$ -1212) superconductor. We will study the mechanism, which enhances  $T_c(0)$  with the optimization of carriers in  $\text{CuO}_2$  planes. We have measured fluctuation-induced conductivity (FIC) of  $\text{Cu}_{0.5}\text{Tl}_{0.5}$ -1212 superconductor thin films to study such a mechanism. The thermal fluctuations in high temperature superconductors give a finite probability of forming Cooper pairs well above  $T_c$ , which induce excess conductivity during the transport of carriers [7–9]. There are two contributions to the FIC in oxide superconductors, one arises from the formation of Cooper pairs

using thermal fluctuations well above  $T_{c,\text{onset}}$  and which has 3D characteristics whereas the second contribution originates from the 2D character of the carrier transport due to the interaction of the Cooper pairs with the already existing normal electrons [10–12]. There are two main theories describing the origin of fluctuations during the formation of Cooper pairs in high temperature superconductors. These are the Aslamazov–Larkin (AL) and Lawrence–Doniach (LD) theories [13, 14]; the Maki–Thomson (MT) corrections are absent in high temperature superconductors due to pair breaking effects that arise from inelastic electron scattering [15].

According to the AL theory, the excess conductivity ' $\sigma'$ ' of the carriers is given by  $\sigma' = C_F^{2D} \varepsilon^{-1}$  for 2D and  $\sigma' = C_F^{3D} \varepsilon^{-1/2}$  for 3D behavior, where  $\varepsilon = (T/T_c) - 1$  is the reduced temperature whilst  $C_F^{2D} = (e^2/16\hbar d)$  and  $C_F^{3D} = [e^2/32\hbar\xi_c(0)]$  are the fluctuation amplitudes in two and three dimensions, respectively [16–19]. In these relations  $e$ ,  $d$  and  $\xi_c(0)$  are the electronic charge, interlayer thickness and  $c$ -axis coherence length, respectively. The aforementioned theories of fluctuation conductivity are used to study the dimensionality of the fluctuations associated with the order parameter of the superconductor [20–22]. From these studies the microscopic parameters such as coherence length could be estimated [7–9, 13]. In oxide superconductors (with low

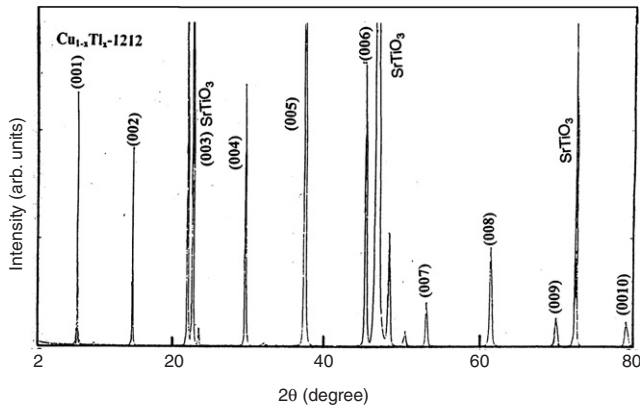


**Figure 1.** X-ray diffraction pattern of as-prepared  $\text{Cu}_{0.5}\text{Tl}_{0.5}\text{-1212}$  superconductor thin film.

anisotropy) at low temperatures there is a transition from 2D to 3D behavior of fluctuations. The temperature at which this cross-over takes place is denoted by  $T^o$  and is related to  $\varepsilon^o$ ; at  $T^o$  the  $c$ -axis coherence length  $\xi_c(0) \sim d$  ( $d$  being the interlayer thickness) and  $\varepsilon^o = (T^o/T_c) - 1$  [23].

There are two important parameters for the analysis of the fluctuation-induced conductivity. The first one is based on the calculation of normal state resistivity [24–26] and second parameter relies on the correct choice of critical temperature,  $T_c$  [8, 9, 23, 27–29]. We have adopted the following method to calculate the excess conductivity,  $\sigma' = 1/\rho - 1/\rho_n$ ; where  $\rho$  is the measured resistivity and  $\rho_n$  is the normal state resistivity extrapolated to absolute zero of temperature. The normal state resistivity was calculated by using  $\rho_n = AT + B$ . The coefficients  $A$  and  $B$  are determined by fitting the data to this equation. In previous studies of FIC the  $\rho_n$  was calculated by fitting the data in the temperature range well above  $T_c$  where the variation of resistivity with temperature was linear; in the analysis of our results we have followed the same procedure [21, 26]. The second most important parameter for the analysis of excess conductivity is the correct choice of  $T_c$ , since it arises in the  $(\ln \sigma' \text{ versus } \ln[(T/T_c) - 1])$  expression. A few authors have chosen the mid point temperature of the resistive transition [28], whereas others have selected the zero resistivity temperature to establish  $T_c$  [29]. We have used the peak temperature from  $d\rho/dT$  plots to determine  $T_c$ , in line with the majority of authors [8, 9, 13, 27, 28]. This choice is more appropriate for polycrystalline superconductors because the complete zero resistivity state in these materials is achieved at lower temperatures when the grains are completely coupled together, whereas the grains themselves become superconducting at relatively higher temperatures [28, 29].

The  $\text{Cu}_{0.5}\text{Tl}_{0.5}\text{-1212}$  superconductors have a  $\text{Cu}_{0.5}\text{Tl}_{0.5}\text{Ba}_2\text{O}_{4-\delta}$  charge reservoir layer and crystallographically equivalent  $\text{CuO}_2$  planes (only outer planes), resulting in a homogeneous distribution of carriers there [30, 31]. This uniform carrier distribution in the conducting  $\text{CuO}_2$  planes gives a symmetrical shape to the Fermi surface. Hence the possible effects arising from the inhomogeneous distribution of carriers and their intrinsic effects on the superconductivity of  $\text{Cu}_{0.5}\text{Tl}_{0.5}\text{-1212}$

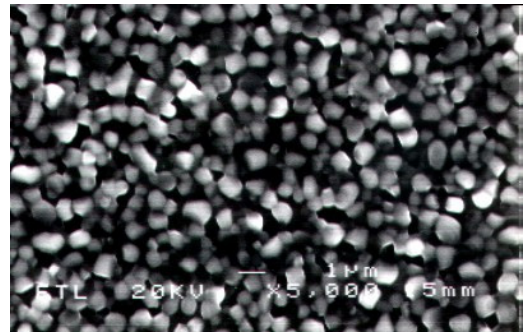


**Figure 2.** Electron micrograph of one of the  $\text{Cu}_{0.5}\text{Tl}_{0.5}\text{-1212}$  thin film samples.

thin films is eliminated, making these films ideal for the study of 2D and 3D behavior in oxide superconductors.

## 2. Experimental details

The  $\text{Cu}_{0.5}\text{Tl}_{0.5}\text{-1212}$  thin films were prepared at normal pressure using an amorphous phase epitaxy method (APE). In this method the  $\text{Cu}_{0.5}\text{Ba}_2\text{CaCu}_2\text{O}_{8-\delta}$  amorphous phase was deposited on a  $\text{SrTiO}_3$  substrate by rf-sputtering at the first stage then treating it with a precursor pellet containing thallium in the second stage at  $860^\circ\text{C}$ ; the composition of the thallium-containing pellet is  $\text{Cu}_{0.5}\text{Tl}_{0.5}\text{Ba}_2\text{CaCu}_2\text{O}_{8-\delta}$ . Using this technique the amorphous phase of Cu-1212 is transformed to a crystalline superconducting  $\text{Cu}_{0.5}\text{Tl}_{0.5}\text{-1212}$  phase. Thallium oxide in this reaction process acts as a structure stabilizer and accelerator of the reaction rate. The structure of the film was determined by XRD, surface roughness by electron microscopy and the composition analysis by EDX measurements. The post-annealing experiments were done in a tubular furnace using 99.99% pure oxygen and nitrogen for 2 h. The resistivity measurements were carried out using the four-probe method. For resistivity measurements, sputter deposited gold contacts were made on the surface of films by a DC-sputtering method using a DC power of  $50 \text{ W cm}^{-2}$ . These contacts had a contact resistivity of  $10^{-9} \Omega \text{ cm}$  [32]. The composition of thin films determined by energy dispersive x-ray (EDX) spectroscopy is  $\text{Cu}_{0.5}\text{Tl}_{0.5}\text{Ba}_2\text{Ca}_1\text{Cu}_2\text{O}_{8-\delta}$ .

## 3. Results and discussion

The XRD of one of the representative sample  $\text{Cu}_{0.5}\text{Tl}_{0.5}\text{-1212}$  thin films prepared at  $860^\circ\text{C}$  is shown in figure 1; all  $(00l)$  lines are showing  $c$ -axis oriented material. The  $c$ -axis length calculated from these lines is  $12.01 \text{ \AA}$ . The quality of the thin films was determined by electron microscopy. The electron micrograph of one of the thin film samples shows a uniform distribution of grains (figure 2). The resistivity measurements of  $\text{Cu}_{0.5}\text{Tl}_{0.5}\text{-1212}$  thin film samples post-annealed at  $400$ ,  $500$  and  $600^\circ\text{C}$  in a nitrogen atmosphere are shown in figure 3. It can be seen from this figure that  $T_c(0)$  which was below  $77 \text{ K}$  in the as-prepared sample is increased to  $91.3 \text{ K}$  after post-annealing at  $400^\circ\text{C}$  but after  $500^\circ\text{C}$  annealing it is decreased to  $89.2 \text{ K}$ . However, after post-annealing at  $600^\circ\text{C}$ ,  $T_c(0)$

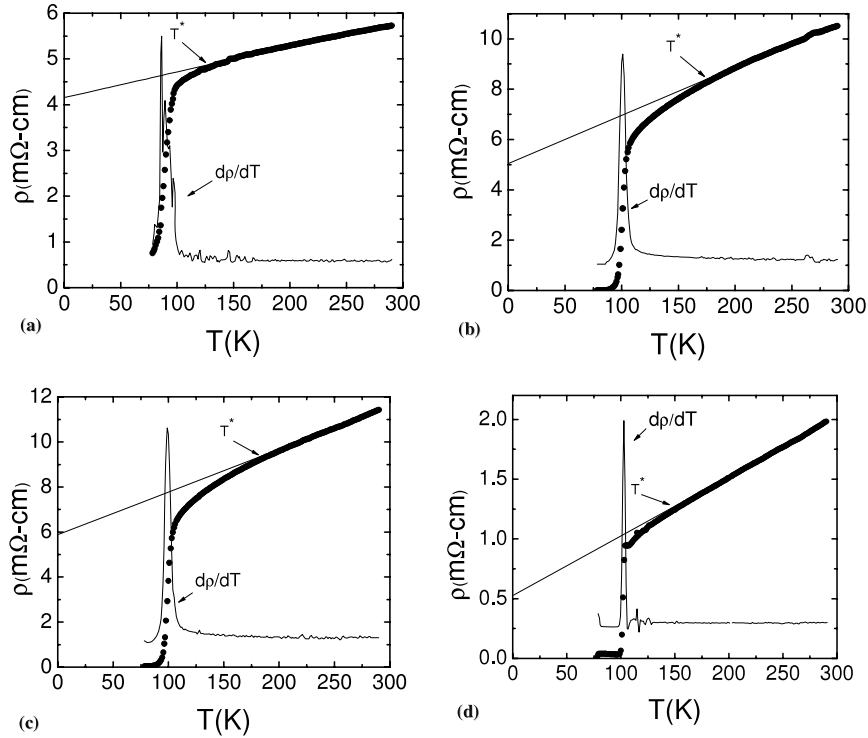


**Figure 3.** Resistivity measurements and  $d\rho/dT$  plot of  $\text{Cu}_{0.5}\text{Tl}_{0.5}\text{-1212}$  superconductor: (a) as-prepared; and post-annealed in nitrogen at 400 °C (b), 500 °C (c) and 600 °C (d).

is again enhanced and a complete superconducting state is achieved at 100 K. The room temperature resistivity ( $\rho_o$ ), first increases with the increase of the post-annealing temperature, but after 600 °C annealing  $\rho_o$  is decreased. In the  $\text{Cu}_{0.5}\text{Tl}_{0.5}\text{-1212}$  superconductor the carrier concentration is controlled by the self-doping mechanism. The self-doping mechanism depends on the oxidation state of the thallium ion in the  $\text{Cu}_{0.5}\text{Tl}_{0.5}\text{Ba}_2\text{O}_{4-\delta}$  charge reservoir layer. When the as-prepared sample is post-annealed in a nitrogen atmosphere at 400 °C the oxygen is removed from the charge reservoir layer, which in turn decreases the density of holes in  $\text{CuO}_2$  planes and their concentration approaches the optimum value which results in an increase in the critical temperature. However, lowering of  $T_c(0)$  after 500 °C annealing could possibly be due to the mixed valence state of copper ( $\text{Cu}^{3+}$ ,  $\text{Cu}^{2+}$ ,  $\text{Cu}^{1+}$ ), which decreases the hole density below the optimum level. But the post-annealing at 600 °C possibly changes the oxidation state of thallium from 3+ to 1+, due to which the lost carriers are recovered in  $\text{CuO}_2$  planes and  $T_c(0)$  is again increased [33, 34]. Moreover, the resistivity versus temperature curve deviates from metallic behavior at a certain temperature,  $T^*$ . One possible source of the deviation of  $\rho$  from linear behavior is the start of some new type of scattering process which leads to the opening of the pseudo-gap (PG) regime. Transition to the PG regime is attributed to the formation of Cooper pairs at temperature  $T > T_c$  and their phase coherence below  $T_c$  [10, 11, 35].

The resistivity measurements of  $\text{Cu}_{0.5}\text{Tl}_{0.5}\text{-1212}$  thin film samples post-annealed at 400, 500 and 600 °C in an oxygen atmosphere are shown in figure 4. The zero resistivity state

was achieved only after post-annealing at 400 and 600 °C;  $\rho_o$  is least in the 400 °C annealed sample. In cuprate high  $T_c$  superconductors the critical temperature depends on the carrier concentration which is a function of the amount of oxygen in the charge reservoir layer. The increase in critical temperature of nitrogen annealed samples is higher than in oxygen annealed samples, showing that nitrogen annealing brings the carrier concentration close to the optimum level. From figure 5 the zero resistivity critical temperature also seems to be correlated with room temperature resistivity ( $\rho_o$ );  $\rho_o$  of the nitrogen annealed sample is higher than for the oxygen annealed sample. This could be due to the removal of oxygen from the intergranular regions of nitrogen annealed samples. The removal of oxygen from the intergranular regions lowers the conductivity of grain boundary junctions. During the resistivity measurements the main source of resistance to the carriers is the grain boundaries. In polycrystalline high temperature superconductors the critical temperature of the grains is higher than for grain boundary junctions. The complete zero resistivity state is achieved only when these junctions become superconducting [28]. The increase in  $T_c(0)$  with the decrease of room temperature resistivity could be due the enhancement of critical temperature of the grain boundary junctions. This is the extrinsic source of increase in critical temperature. Therefore, the sources of  $T_c(0)$  enhancement/suppression in these  $\text{Cu}_{0.5}\text{Tl}_{0.5}\text{-1212}$  superconductor samples are both intrinsic and extrinsic.

The temperature dependence of  $d\rho/dT$  of nitrogen and oxygen annealed samples is also shown in figures 3 and 4. These figures show that the  $d\rho/dT$  plot of the as-prepared

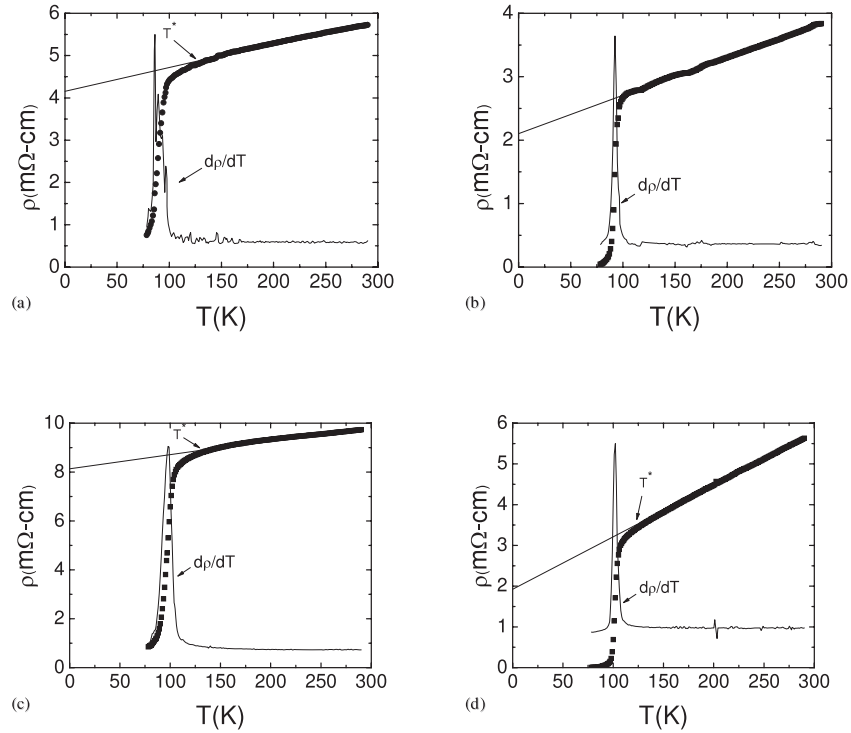


**Figure 4.** Resistivity measurements and  $d\rho/dT$  plot of  $\text{Cu}_{0.5}\text{Tl}_{0.5}\text{-1212}$  superconductor: (a) as-prepared; and post-annealed in oxygen at 400 °C (b), 500 °C (c) and 600 °C (d).

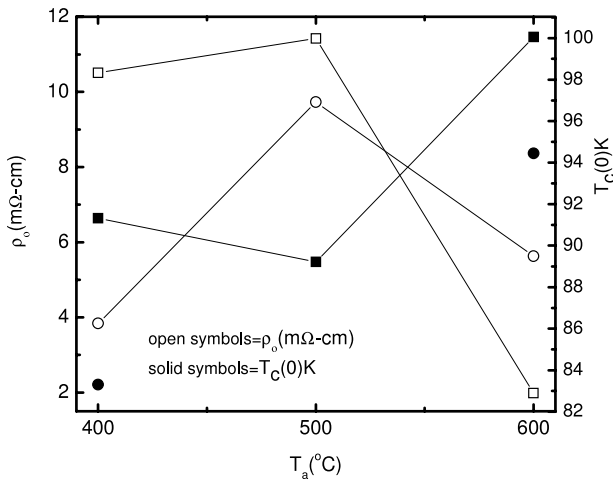


**Figure 5.**  $\rho_o$  and  $T_c(0)$  (squares, nitrogen annealed; circles, oxygen annealed) versus annealing temperature of  $\text{Cu}_{0.5}\text{Tl}_{0.5}\text{-1212}$  superconductor thin films.

sample has more than one peak which may be due to the presence of some weak links between the grains. But after post-annealing well defined  $d\rho/dT$  peaks are achieved, which shows that post-annealing has improved the quality of the films which is also observed from lowering of the room temperature resistivity after post-annealing [36]. Though the value of  $\rho_o$  is smaller in oxygen-annealed samples compared to nitrogen annealed samples, the critical temperature is higher in nitrogen annealed sample showing that the dominant contribution to superconductivity is from intragranular regions due to a change in carrier concentration in  $\text{CuO}_2$  planes compared to the grain

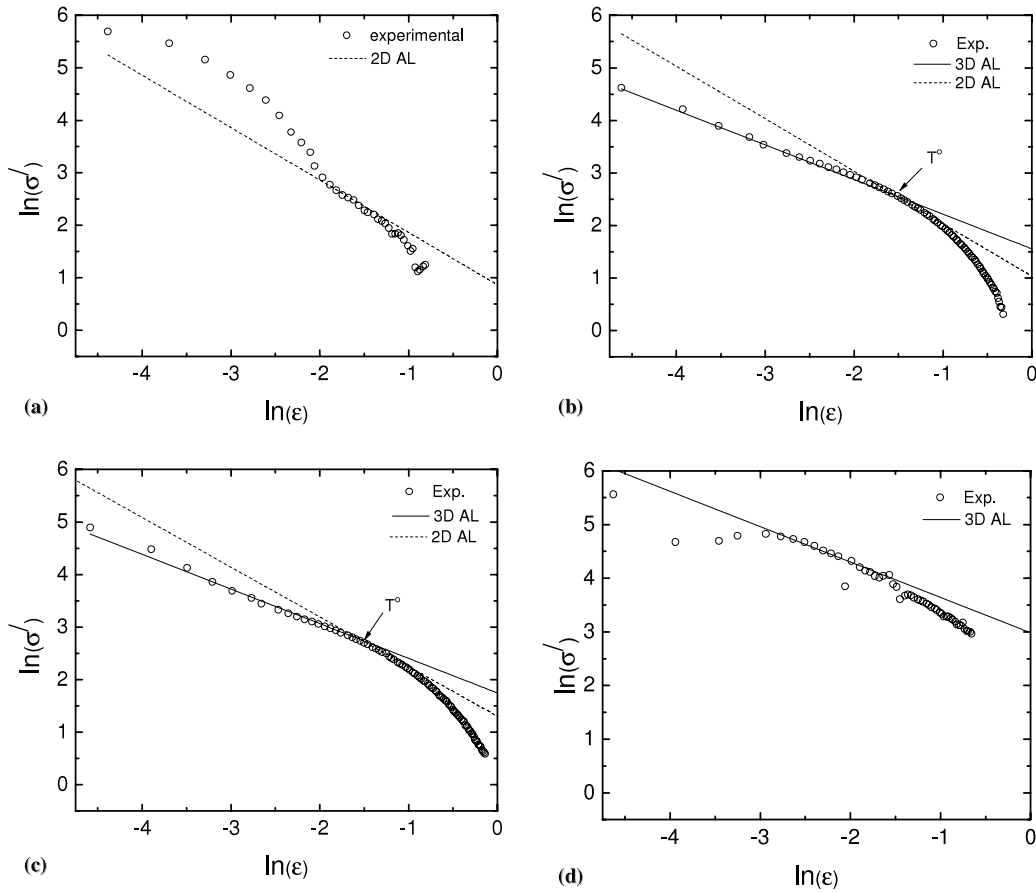
**Table 1.**  $T_{c,\text{mid}}$  and  $T_c(0)$  of nitrogen and oxygen post-annealed samples.

Annealing temperature (°C)	N <sub>2</sub> -annealing		O <sub>2</sub> -annealing	
	$T_{c,\text{mid}}$ (K)	$T_c(0)$ (K)	$T_{c,\text{mid}}$ (K)	$T_c(0)$ (K)
As-prepared	86.012	<77	86.012	<77
400	101.057	91.32	92.366	83.309
500	99.044	89.213	98.03	<77
600	102.056	100.053	102.056	94.443

boundaries. The values of  $T_{c,\text{mid}}$ , which is the peak temperature of the  $d\rho/dT$  plot, and  $T_c(0)$  are given in table 1.

We have also determined the excess conductivity induced by thermal fluctuations in  $\text{Cu}_{0.5}\text{Tl}_{0.5}\text{-1212}$  superconductor thin films after post-annealing in nitrogen and oxygen atmospheres. We have analyzed the fluctuation-induced conductivity (FIC) of  $\text{Cu}_{0.5}\text{Tl}_{0.5}\text{-1212}$  superconductor thin films using standard AL theory. The analysis of FIC provides information about the dimensionality of the fluctuations associated with the order parameter of the Cooper pairs. In the previous studies of FIC of  $\text{Cu}_{0.5}\text{Tl}_{0.5}\text{-1234}$  superconductor thin films we observed that the critical temperature is increased with the increase of the width of the 3D region of paraconductivity [37]. We have calculated  $\sigma'$  of  $\text{Cu}_{0.5}\text{Tl}_{0.5}\text{-1212}$  thin films in the temperature range from  $T^*$  (pseudo-gap temperature) down to 77 K. This choice of temperature range for FIC analysis is appropriate because Cooper pair formation takes place in this temperature range. The results of FIC of nitrogen annealed samples are shown in figure 6; the as-prepared sample for such studies is also included for comparison. It can be seen from this





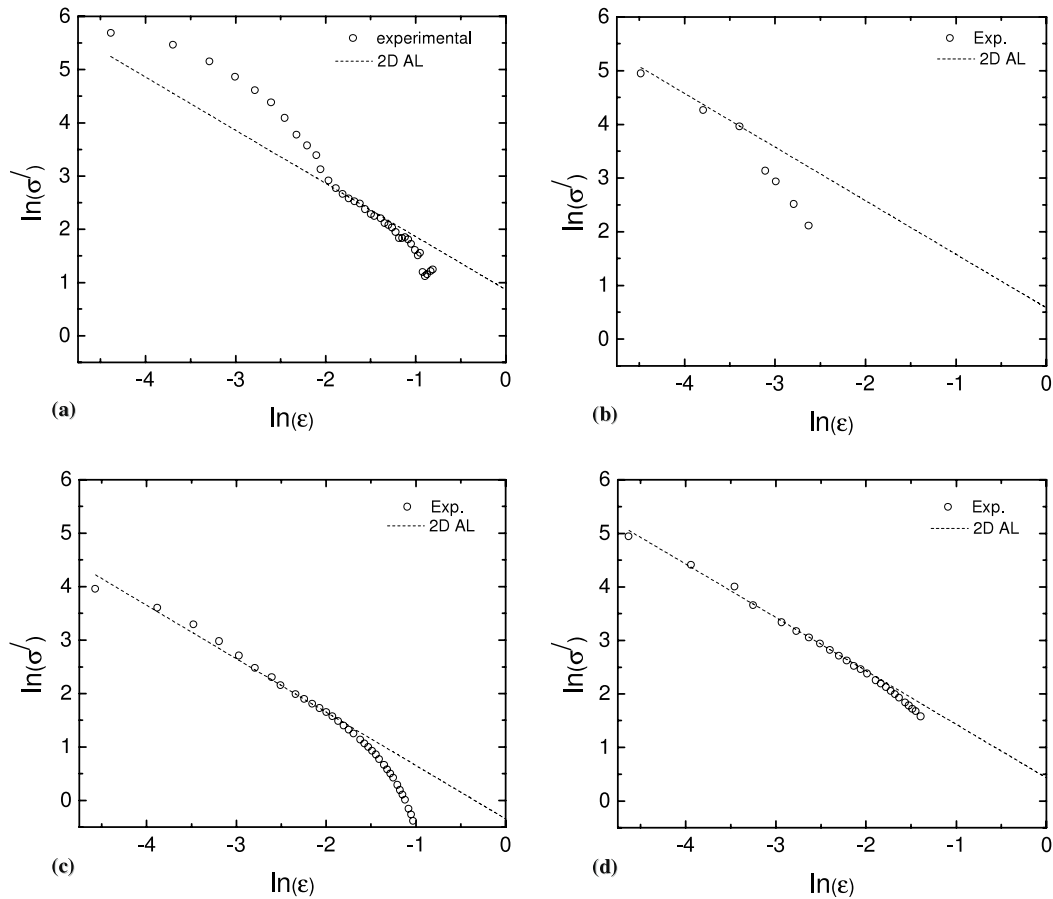
**Figure 6.**  $\ln$ - $\ln$  plot of fluctuation-induced conductivity of  $\text{Cu}_{0.5}\text{Tl}_{0.5}$ -1212 superconductor thin films: (a) as-prepared; and post-annealed in nitrogen at 400 °C (b), 500 °C (c), 600 °C (d). The solid line (3D-AL), dashed line (2D-AL) and open circles represent experimental data.

figure that the as-prepared sample shows only 2D fluctuations in the higher temperature region which gives rise to excess conductivity (figure 6(a)). But after post-annealing in nitrogen at 400 and 500 °C a transition from the 2D to the 3D regime is observed which extends over a wide temperature range in the low temperature region (figures 6(b) and (c)). The 2D–3D cross-over temperatures  $T^\circ$  are 122 K and 121 K in 400 and 500 °C samples, respectively. In the case of the 600 °C sample, which has a higher critical temperature, no sign of 2D fluctuations is observed but 3D fluctuations are present (figure 6(d)). It could also be seen from this figure that width of the 3D region of fluctuations extends over a wide temperature range as  $T_c(0)$  increases. These results show that three-dimensional thermal fluctuations bring the critical temperature to higher values. In addition, from figure 5 a direct correlation between  $\rho_o$  and  $T_c(0)$  is observed, which shows that thermally induced conductivity also depends on the nature of grain boundaries. In the previous results for post-annealing of  $\text{Cu}_{0.5}\text{Tl}_{0.5}$ -1234 superconductor thin films in a nitrogen atmosphere we observed an increase in the grain size along with enhancement of  $T_c(0)$  and  $T^\circ$ . The grain size plays an important role because with the increase of grain size of the sample the number of grain boundaries which act as a source of scattering to the mobile carriers is decreased [37]. The decreased scattering of the carriers possibly gives rise to three-dimensional fluctuation-induced conductivity.

The measurements of FIC of  $\text{Cu}_{0.5}\text{Tl}_{0.5}$ -1212 thin films post-annealed in oxygen are shown in figure 7. These results show that the  $\sigma'$  data only satisfy the 2D-AL theory and the 3D fluctuations are absent altogether in these samples. There could be two possible reasons for the absence of 3D fluctuations which keep  $T_c(0)$  of these samples below that of nitrogen annealed samples. One is the carrier concentration below optimum level and second is the smaller grain size as compared to the nitrogen annealed samples. Although the inter-grain connectivity of oxygen annealed samples seems better than that of nitrogen annealed samples it would not be sufficient to facilitate the transport of mobile carriers through the grain boundaries without any dissipation of energy.

#### 4. Conclusions

We conclude from the preceding results that the zero resistivity critical temperature of  $\text{Cu}_{0.5}\text{Tl}_{0.5}$ -1212 superconductor thin films largely depends on the dimensionality of thermal fluctuations which induce excess conductivity in these samples. There are two sources which affect the dimensionality of fluctuations; one is the intrinsic properties of intragrain regions, i.e. the carrier concentration in  $\text{CuO}_2$  planes, and the second is the nature of the grain boundary junctions and the grain size (extrinsic properties). The nitrogen annealed samples with higher  $T_c(0)$  and higher  $\rho_o$  possess



**Figure 7.**  $\ln$ - $\ln$  plot of fluctuation-induced conductivity of  $\text{Cu}_{0.5}\text{Tl}_{0.5}$ -1212 superconductor thin films: (a) as-prepared; and post-annealed in oxygen at 400 °C (b), 500 °C (c) and 600 °C (d). The dashed line (2D-AL) and open circles represent experimental data.

3D type fluctuations, while in the oxygen annealed samples even the grain boundaries seems to be good, but due to the absence of an optimized carrier concentration in  $\text{CuO}_2$  planes and possibly a smaller grain size only 2D fluctuations are observed. Therefore, we can conclude that the optimum carrier concentration, the strong connectivity of grains and the large grain size are possible sources of 3D fluctuations which ultimately bring the critical temperature to higher values. Since the mechanism of  $T_c(0)$  variation in high temperature superconductors is not yet clear, such types of measurements would help us to explore the underlying phenomenon.

## Acknowledgment

Pakistan Science Foundation [PSF/Res/C-QU/PHYS (122)] is acknowledged for its financial support.

## References

- [1] Ihara H, Sekita Y, Tateai H, Khan N A, Ishida K, Harashima E, Kojima T, Yamamoto H, Tanaka K, Tanaka Y, Terada N and Obara H 1999 *IEEE Trans. Appl. Supercond.* **9** 1551
- [2] Wijngaarden R J, Jover D T and Griessen R 1999 *Physica B* **265** 128
- [3] Karppinen M and Yamauchi H 1999 *Phil. Mag.* **B 79** 343
- [4] Yamauchi H and Karppinen M 1999 *J. Low Temp. Phys.* **117** 813
- [5] Tokunaga Y, Ishida K, Kitaoka Y, Asayama K, Tokiwa K, Iyo A and Ihara H 2000 *Phys. Rev. B* **61** 9707
- [6] Zhang H and Sato H 1993 *Phys. Rev. Lett.* **70** 1697
- [7] Han S H, Lundqvist P and Rapp Ö 1997 *Physica C* **282** 1571
- [8] Han S H, Bryntse I, Axnäs J, Zhao B R and Rapp Ö 2004 *Physica C* **408** 679
- [9] Han S H, Bryntse I, Axnäs J, Zhao B R and Rapp Ö 2003 *Physica C* **388** 349
- [10] Solovjov A L, Hambermeier H-U and Haage T 2002 *Low. Temp. Phys.* **28** 17
- [11] Solovjov A L, Hambermeier H-U and Haage T 2002 *Low. Temp. Phys.* **28** 99
- [12] Mun M, Lee S, Salk S S, Shin H J and Joo M K 1993 *Phys. Rev. B* **48** 6703
- [13] Kim D H and Goldman A M 1989 *Phys. Rev. B* **39** 12275
- [14] Ghosh A K, Bandyopadhyay S K and Basu A N 1999 *J. Appl. Phys.* **86** 3247
- [15] Pradhan A K, Roy S B, Chaddah P, Chen C and Wanklyn B M 1994 *Phys. Rev. B* **50** 7180
- [16] Mun M, Lee S, Salk S S, Shin H J and Joo M K 1993 *Phys. Rev. B* **48** 6703
- [17] Han S H and Rapp Ö 1995 *Solid State Commun.* **94** 661
- [18] Juang J Y, Hsieh M C, Luo C W, Uen T M, Wu K H and Gou Y S 2000 *Physica C* **329** 45
- [19] Sato T, Nakane H, Yoshizawa S and Mori N 2001 *Physica C* **372** 1208
- [20] Vidal F, Veira J A, Maza J, Garcia-Alvarado F, Moran E and Alario M A 1999 *J. Phys. C: Solid State Phys.* **21** L599
- [21] Han S H, Eltsev Yu and Rapp Ö 2000 *Phys. Rev. B* **61** 11776
- [22] Azzouz F B, Zouaoui M, Annabi M and Salem M B 2006 *Phys. Status Solidi* **3** 3048

- [23] Mori N and Satoh H 2004 *Physica C* **412** 1310
- [24] Sato T, Nakane H, Mori N and Yoshizawa S 2001 *Physica C* **357** 244
- [25] Satoh H, Tanabe T, Nakane H, Yoshizawa S and Mori N 2004 *Physica C* **412** 307
- [26] Han S H, Eltsev Yu and Rapp Ö 1998 *Phys. Rev. B* **57** 7510
- [27] Han S H, Lundqvist P and Rapp Ö 1997 *Physica C* **282** 1571
- [28] Patapis S K, Jones E C, Phillips J M, Norton D P and Lowndes D H 1995 *Physica C* **244** 198
- [29] Nayak P K and Ravi S 2006 *Solid State Commun.* **140** 464
- [30] Hamada N and Ihara H 2001 *Physica C* **357** 108
- [31] Tokunaga Y, Ishida K, Kitaoka Y, Asayama K, Tokiwa K, Ayo A and Ihara H 2000 *Phys. Rev. B* **61** 9707
- [32] Harashima E, Khan N A, Sekita Y, Ishida K and Ihara H 2002 *Supercond. Sci. Technol.* **15** 29
- [33] Tanaka K, Iyo A, Terada N, Tokiwa K, Miyashita S, Tanaka Y, Tsukamoto T, Agarwal S K, Watanabe T and Ihara H 2001 *Phys. Rev. B* **63** 64508
- [34] Ihara H, Tanaka K, Tanaka Y, Iyo A, Terada N, Tokumoto M, Ariyama M, Tateai F, Kawamura M, Ishida K, Miyashita M and Watanabe T 2000 *Physica B* **284** 1085
- [35] Juang J Y, Hsieh M C, Luo C W, Uen T M, Wu K H and Gou Y S 2000 *Physica C* **329** 45
- [36] Juang J Y, Hsieh M C, Luo C W, Uen T M, Wu K H and Gou Y S 2000 *Physica C* **329** 45
- [37] Khurram A A, Mumtaz M, Khan N A, Ahadian M M and Iradj-zad A 2007 *Supercond. Sci. Technol.* **20** 742